Unique Guest-Inclusion Properties of a Breathing Ionic Crystal of $K_3[Cr_3O(OOCH)_6(H_2O)_3][\alpha\text{-}SiW_{12}O_{40}]\cdot 16H_2O$

Sayaka Uchida and Noritaka Mizuno*[a]

Abstract: A microstructured ionic crystal, $K_3[Cr_3O(OOCH)_6(H_2O)_3][\alpha\text{-}SiW_{12}O_{40}]\cdot 16H_2O$ (**1**) was synthesized by the complexation of the Keggin-type polyoxometalate of $[\alpha\text{-}SiW_{12}O_{40}]^{4-}$ with a macrocation of $[Cr_3O(OOCH)_6(H_2O)_3]^+$. Compound **1** possessed a straight channel, with an opening of approximately 0.5×0.8 nm, which contained the water of crystallization. The use of the macrocation with large size (0.7 nm) and small charge (+1) reduced the anion–cation interaction and was essential for the channel formation. The molecular structures of the polyoxometalate and the macrocation in **1** were retained under vacuum at 473 K. Analogues of **1** were synthesized with $[\alpha\text{-}PVW_{11}O_{40}]^{4-}$ or $[Fe_3O(OOCH)_6(H_2O)_3]^+$. The water of crystallization in **1** was removed under vacuum at room temperature to form the closely packed guest-free phase **2**. Compound **2** reversibly and repeatedly included water and polar organic molecules with two carbon atoms or less. Guest inclusion was highly selective and a difference of even one methylene group in the organic guest molecule was discriminated by the host. Polar organic molecules with longer methylene chains and nonpolar molecules such as dinitrogen and methane were completely excluded. The guest-inclusion properties could be explained by the ion–dipole interaction between the host and the guest, which is proportional to the dipole moment of the guest molecule and inversely proportional to the ion–dipole (host–guest) distance. Thus, small polar molecules were selectively absorbed. These distinctive guest-inclusion properties were successfully applied to the oxidation of methanol from a mixture of C_1 and C_2 alcohols. These results show unique guest inclusion and catalysis by rationally designed ionic crystals.

Keywords: host–guest systems · polyoxometalates · selective sorption · thermodynamics

Introduction

Crystalline microstructured materials such as zeolites possess molecule-sized spaces in their lattice and have attracted considerable attention owing to their guest-inclusion properties. Inorganic aluminosilicate zeolites are composed of covalently bonded $[TO_4]$ units with structurally rigid micropores. There is a long history of research into such materials.[1] Currently there is great interest in the synthesis of self-organized supramolecular complexes. A wide variety of complexes have been synthesized by the incorporation of organic groups and these complexes are expected to display unique guest-inclusion properties and catalysis.[2] In this context, these supramolecular complexes are often called "organic zeolites".[3] The guest molecules are included with specific interactions such as coordination bonds,[4] hydrogen bonds,[5] or aromatic interactions.[6] Therefore, organic zeolites often exhibit unique guest-inclusion properties and the three-dimensional arrangements of the constituent molecules are apt to change with the type and amount of the guests.[2e, 3a, 5, 6b]

There are some examples of catalysis (for example, cyanosilylation,[2a] photochemical reactions,[2g] selective esterification,[2c] and oxidation of sulfides[2f]) by supramolecular complexes and the guest-inclusion properties in these systems have been extensively studied. However, scarcely anything is known about the size-selective oxidation of alcohols by such complexes. The incorporation of catalytically active sites or molecules into the crystal lattice of the microstructure could lead to the development of novel catalysts in this area.

Polyoxometalates are discrete metal–oxygen cluster anions and possess redox or acid–base properties.[7] In addition, some polyoxometalates in the solid state show sorption properties or have micropores. For example, an acid-form polyoxometalate compound, $H_3PW_{12}O_{40}$, absorbs polar mol-

[a] Prof. Dr. N. Mizuno, Dr. S. Uchida
Department of Applied Chemistry
School of Engineering
The University of Tokyo
7-3-1 Hongo, Bunkyo-ku, Tokyo 113-8656 (Japan)
Fax: (+81) 3-5841-7220
E-mail: tmizuno@mail.ecc.u-tokyo.ac.jp

Supporting information for this article is available on the WWW under http://www.chemeurj.org/ or from the author.

DOI: 10.1002/chem.200304874

ecules into the solid bulk in a nonselective way and then acid-catalyzed reactions proceed in the bulk.[8] On the other hand, the substitution of H^+ with Cs^+ renders the compound insoluble and produces micropores between the nanocrystallites. Acid or oxidation reactions proceed in the micropores in a shape-selective manner.[9] Nanosized polyoxometalates are also suitable building blocks for crystalline microstructured materials[10] and some of these compounds contain nitriles or alcohols as guests,[11] although they can not be removed or reversibly included.

We have preliminarily communicated the selective and reversible guest inclusion of alcohols and nitriles smaller than C_3 by an ionic crystal of $K_3[Cr_3O(OOCH)_6(H_2O)_3][\alpha\text{-}SiW_{12}O_{40}]\cdot 16H_2O$ (**1**).[12] Herein, we report the full details of the synthesis and crystal structure of **1**, the guest-inclusion properties of the guest-free phase **2**, and the investigation of the physico-chemical factors controlling the highly selective inclusion of polar organic molecules with two carbon atoms or less. The nature of the guest inclusion of **2** can be explained by the magnitude of the ion–dipole interaction between the host and guest. The distinctive guest-inclusion properties of **2** have been applied to the size-selective oxidation of a mixture of C_1 and C_2 alcohols. The results show novel guest inclusion and catalysis by rationally designed ionic crystals.

Results and Discussion

Synthesis, crystal structure, and stability of 1: Figure 1 depicts the synthesis and the crystal structure of **1** (*ab* and *ac* planes). The molecular structures of $[\alpha\text{-}SiW_{12}O_{40}]^{4-}$[13] (polyoxometalate) and $[Cr_3O(OOCH)_6(H_2O)_3]^+$[14] (macrocation) in **1** agreed with previous reports. As shown in Figure 1, the polyoxometalates and macrocations lined up alternately along the *c* axis to form a column and three potassium ions compensated for the minus charge. The columns were hexagonally placed to construct a straight channel with an opening of approximately 0.5×0.8 nm (36% of the unit cell).[15] The large size and the small charge of the ions (polyoxometalate: size ≈ 1.0 nm, charge $=-4$; macrocation: size ≈ 0.7 nm, charge $=+1$) reduced the ion–ion interaction and were crucial to the creation of the channel. The bridging formate groups of the macrocation were positioned toward the polyoxometalates and were weakly hydrogen-bonded to the oxygen atoms (O···H–C: 0.324–0.336 nm). The water of crystallization (light blue circles in Figure 1) was positioned in the channel and was in the vicinity of potassium ions (K···O_w: 0.273–0.287 nm) or was hydrogen-bonded to the oxygen atoms of the macrocations (O···O_w: 0.258–0.267 nm) or polyoxometalates (O···O_w: 0.281–0.308 nm). These water molecules were desorbed under vacuum at room temperature to form a closely packed guest-free phase, **2**. Details of the structure and properties of **2** will be described in later sections. Ionic crystals were also synthesized with Keggin-type vanadium-substituted polyoxometalate $[\alpha\text{-}PVW_{11}O_{40}]^{4-}$ or the iron(III) macrocation $[Fe_3O(OOCH)_6(H_2O)_3]^+$. The IR spectra showed characteristic bands for the polyoxometalate and the macrocation, thereby indicating that the molecular structures of the ions were maintained in the ionic crystals. The chemical formulae of the ionic crystals were determined as $K_3[Fe_3O(OOCH)_6(H_2O)_3][\alpha\text{-}SiW_{12}O_{40}]\cdot 16H_2O$ (**3**) and $K_3[Cr_3O(OOCH)_6(H_2O)_3][\alpha\text{-}PVW_{11}O_{40}]\cdot 16H_2O$ (**4**) by elemental analysis (see the Experimental Section). Ionic crystals **3** and **4** showed essentially the same powder X-ray diffraction (XRD) patterns as that of **1**, a fact showing that the anion–cation arrangements were identical to **1** (see Figure S-1 in the Supporting Information).[16]

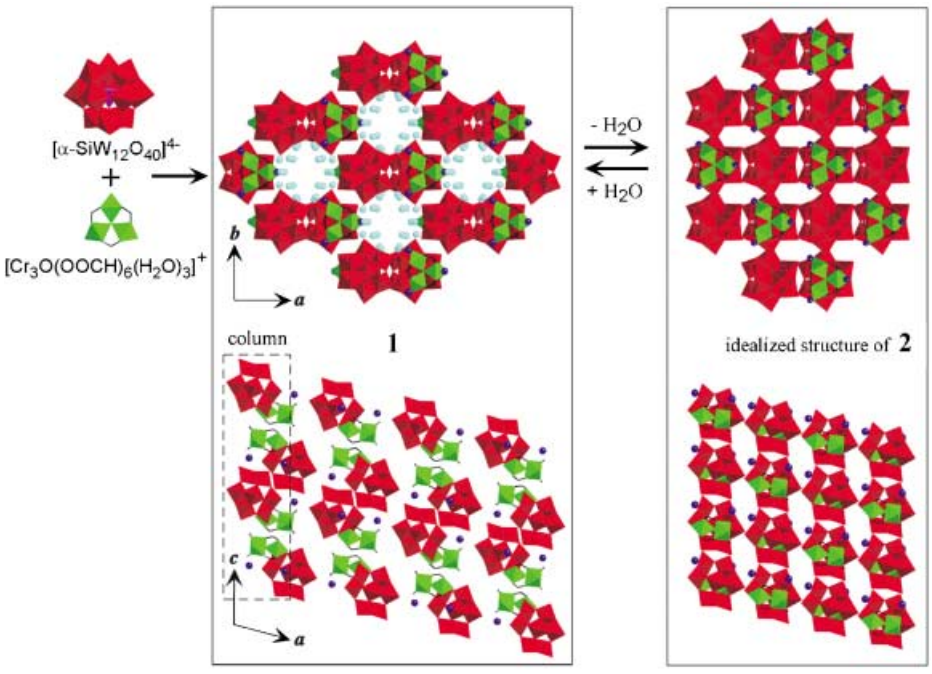

Figure 1. Syntheses and crystal structures (*ab* and *ac* plane) of **1** and **2**. Blue and light blue spheres are K^+ ions and oxygen atoms of the water of crystallization, respectively.

Next, the stability of the constituent ions of **1** was investigated by IR spectroscopy (see Figure S-2 in the Supporting Information). Drying of **1** under vacuum at room temperature to form **2** resulted in a weight loss of 7.6%, which corresponds to 16 molecules of water of crystallization (calcd. 7.6%). The weight loss of **1** under vacuum at 473 K was 9.4%, which is approximately equal to the loss of the water of crystallization together with the 3 molecules of the coordination water of the macrocation (calcd. 9.0%). The IR spectra of **1** under vacuum at 473 K showed the characteristic bands of $[\alpha\text{-}SiW_{12}O_{40}]^{4-}$[17] at around 980 ($\nu_{asym}$(W=O)), 930 ($\nu_{asym}$(Si–O)), 890

(ν_{asym}(W–Oc–W)), and 790 cm^{-1} (ν_{asym}(W–Oe–W)) and those of the macrocation[18] at around 1635 (ν_{asym}(OCO)), 1380 (ν_{sym}(OCO)), and 660 cm^{-1} (ν_{asym}(Cr_3–O)). This fact shows that the molecular structures of the constituent ions were retained up to 473 K. No changes were observed for the characteristic IR bands of $K_4[\alpha\text{-}SiW_{12}O_{40}]$ and $[Cr_3O(OOCH)_6(H_2O)_3](OOCH)$ under vaccum at 473 K, a fact that supports the stability of the structures. The weight loss of **1** under vacuum at 773 K was $>18\,\%$ and the characteristic bands of the macrocation disappeared; this indicates decomposition of the macrocation. The thermogravimetric (TG) measurement of **1** showed a sharp weight loss around 573–623 K due to decomposition of the macrocation, a result which is consistent with the IR data (Figure S-3 in the Supporting Information). The retention of the molecular structures of the constituent ions up to 473 K was also confirmed by the diffuse reflectance UV/Vis spectrum.[19] The IR spectrum of **1** showed a broad band at around 2000–3500 cm^{-1}, which may be attributed to the ν(OH) bands of the water molecules.[20] The band intensity decreased under vacuum and was restored upon exposure of the crystal to water vapor, which suggests reversible sorption/desorption of the water molecules.

Sorption/desorption of water molecules by 1 and 2: Figures 2a and 2b show the XRD patterns of **1** and **2**, respectively.

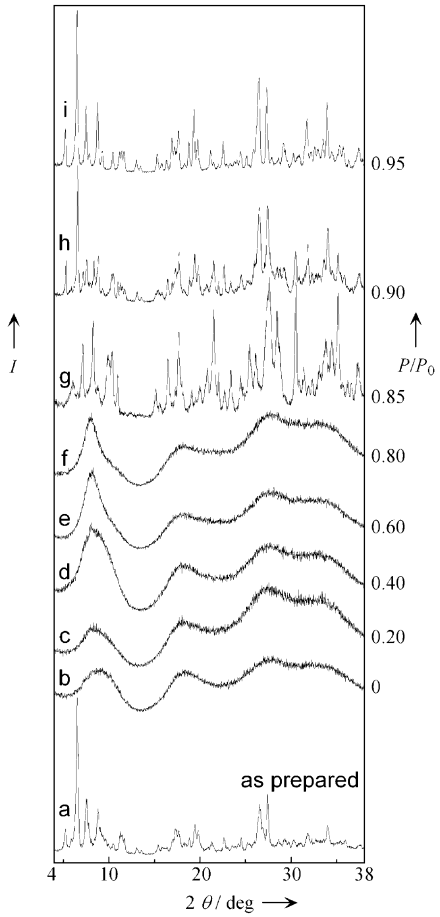

Figure 2. XRD patterns of a) **1** and b) **2**. c)–i) Changes of in situ XRD patterns of **2** with changes in partial pressures of water vapor at 298 K. The water vapor pressure was controlled with N_2 balance.

The distinct peaks of **1** were considerably broadened under vacuum at 298 K, as shown in Figure 2b. The broad pattern is possibly explained by a closest-packing model of the columns, which would be in accord with the low BET surface area (2 $m^2 g^{-1}$) and the fact that **2** showed type-II isotherms for N_2 sorption at 77 K, as is characteristic for nonporous solids.[21] Figures 2c–2i show the changes in the in situ XRD pattern of **2** with exposure to water vapor. An exothermic peak was observed after the increase in the water vapor pressure. At $P/P_0 \leq 0.80$, a broad pattern similar to that in Figure 2b was observed. The diffraction peaks sharpened slightly and shifted to lower angles with the increase in the water vapor pressure, a result indicating lattice expansion of the host solid.[22] A single crystalline phase identical to **1** was formed at and above $P/P_0 = 0.90$.

On the other hand, exposure of **2** to vapors of small polar organic molecules gave XRD patterns different from **1**.[23] These differences show the changes in the anion–cation arrangement with the kind of organic molecules and their inclusion as guests into the solid bulk. Some organic or organometallic complexes exhibit structural transformation upon the inclusion of polar molecules and the structural change can be explained by specific interactions such as hydrogen-bonding between the host and the guest.[2e,3a,5,6b] No changes in the IR and diffuse reflectance UV/Vis bands characteristic of the polyoxometalate and macrocation were observed upon exposure of **2** to vapors of water or organic molecules; this result shows that the molecular structures of the constituent ions are retained.

The water sorption/desorption isotherm of **2** was investigated to quantify the inclusion properties. Figure 3 shows the results at 298 K. For the sorption branch, the amount of water uptake increased monotonically with the vapor pressure and reached approximately 12 molecules per **2** at $P/P_0 \approx 0.8$. The slope became steeper above this point and the uptake reached approximately 18 molecules per **2** at $P/P_0 \approx 0.95$. This number was approximately equal to that of the water of crystallization in **1**. The XRD pattern of the sample after the sorption run was identical to **1**, a result which shows that the water molecules are included into the bulk in the same way as in **1**.

The desorption branch overlapped with the sorption branch at high pressures while a hysteresis existed at low

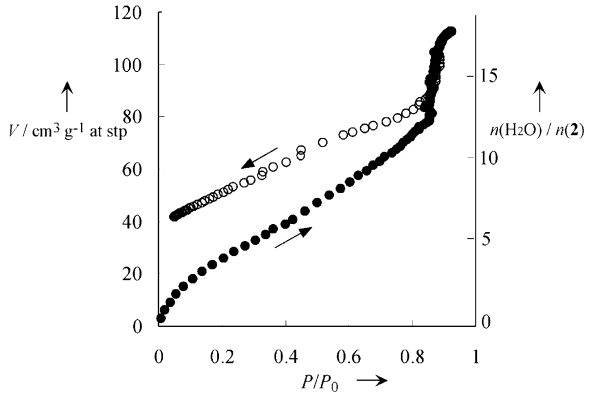

Figure 3. Water sorption/desorption isotherm of **2** at 298 K. Closed and open symbols represent sorption and desorption branches, respectively.

pressures. Similar isotherms of polar absorbents have been reported for montmorillonite. The low-pressure hysteresis has been explained by the specific host–guest interaction (that is, ion–dipole or hydrogen bonding), which alters the crystal structure of the host and allows the guest to escape only very slowly during the desorption run.[24,25] As shown by the light blue circles in Figure 1, the water of crystallization in **1** was in the vicinity of the potassium ions (K···O_w: 0.273–0.287 nm) or was hydrogen-bonded to the oxygen atoms of the macrocations (O···O_w: 0.258–0.267 nm) or polyoxometalates (O···O_w: 0.281–0.308 nm), showing an ion–dipole or hydrogen-bonding interaction. Structural changes (lattice expansion of the host solid) with the inclusion of water molecules were observed as described. Therefore, the water sorption/desorption isotherm of **2** can be explained as follows. Water molecules penetrate and diffuse into the closely packed structure of **2** and the lattice of the ionic crystal expands ($P/P_0 \leq 0.8$). A crystalline phase with a channeled structure, **1**, forms with the completion of the inclusion of water molecules. Water molecules are trapped into the host solid through ion–dipole or hydrogen-bonding interactions and these specific interactions prevent facile desorption and lead to a low-pressure hysteresis. These low-pressure hystereses are different from those for the conventional type-IV isotherms with loops closing at low pressures, due to capillary condensation into mesopores.

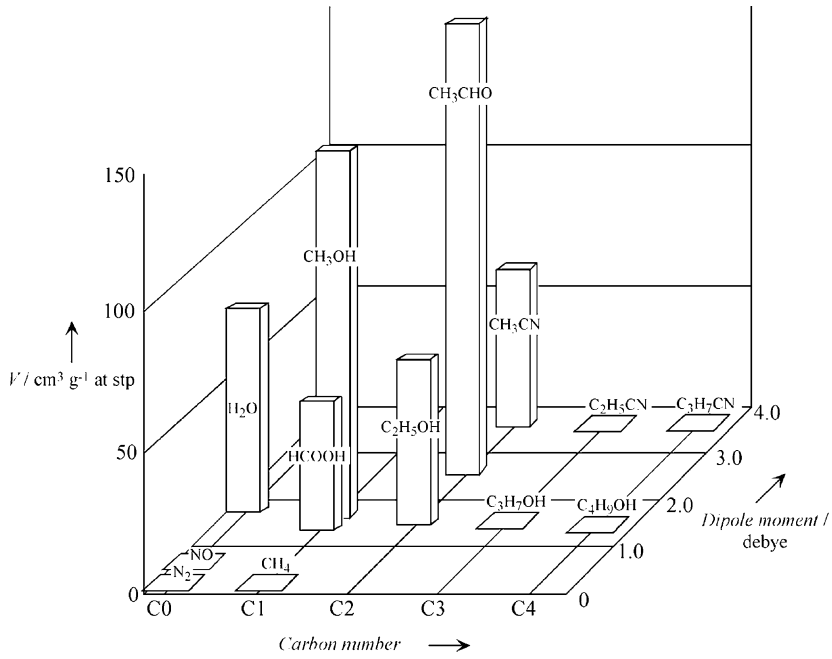

Figure 4. Effect of the number of carbon atoms and the dipole moments of guest molecules on the inclusion properties of **2** at $P/P_0 = 0.8$.

Guest-inclusion properties of 2: The guest inclusion of **2** was investigated with various kinds of molecules. Small polar organic molecules such as acetaldehyde and formic acid were absorbed as well as water, alcohols, and nitriles. Polar organic molecules with longer methylene chains and nonpolar molecules such as dinitrogen and methane were completely excluded. Thus, the guest-inclusion properties of **2** seem to be affected by the number of carbon atoms and the dipole moments[26] of the guest molecules. Only water and the C_1 molecules (methanol and formic acid) were included at a low P/P_0 value of 0.2. Inclusion of C_2 molecules suddenly began at a definite pressure; the existence of such a "gate pressure" in guest inclusion has been reported in several articles.[5e,27] This phenomenon can be explained by the magnitude of the ion–dipole interaction between the host and the guest and by the change in the chemical potential of the guest molecule with the gas pressure, which will be described in the next section. Figure 4 summarizes the results at $P/P_0 = 0.8$. It was clearly shown that the guest-inclusion properties of **2** depended greatly on the number of carbon atoms and the polarity of the guest molecule and that only polar molecules with two carbon atoms or less were included into the solid bulk.

The amounts of inclusion in terms of liquid at $P/P_0 \approx 1$ for water, formic acid, ethanol, and acetonitrile were 0.084, 0.092, 0.157, and 0.140 mL mol^{-1}, respectively. The amounts change with the guests, but values could not be determined for methanol and acetaldehyde due to the irreversible swelling of the host above a P/P_0 value of 0.6. The XRD patterns after the sorption run differed with the guests. Therefore, the differences in the inclusion amounts are probably caused by transformations in the anion–cation arrangements with the inclusion of various guests.

Solid-state magic-angle-spinning (MAS) NMR spectra of **2** loaded with organic molecules were taken to quantify their states. ^{13}C MAS NMR spectra of **2** after the inclusion of six molecules of methanol per **2** exhibited an isotropic peak at $\delta = 57.9$ ppm (methyl carbon) with a half-width of approximately 1.5 kHz and spinning side bands. The position of the isotropic peak showed a lower-field shift of approximately 8 ppm from the $\delta = 50$ ppm signal of the methanol solution. In general, ^{13}C NMR peaks of methanol molecules adsorbed on the surface show much smaller lower-field shifts (< 1 ppm) and are much sharper (half-width < 100 Hz).[28] Therefore, the large lower-field shift and the broadness of the isotropic ^{13}C NMR peak were probably caused by the inclusion of methanol into the host ionic solid.

Investigation of factors controlling the guest-inclusion properties of 2:

Quantitative explanation of the inclusion of small polar molecules: As discussed in a previous section, **2** has a closely

packed structure and the distance among the constituent ions must increase in order to include guests into the solid bulk, as depicted for the water sorption in Figure 2. An energy diagram for the inclusion of guest molecules is schematically shown in Figure 5. If the ion–dipole interaction between the host and the guest (E_{int}) is larger than the energy needed for the solid bulk expansion (E_1) then the guest

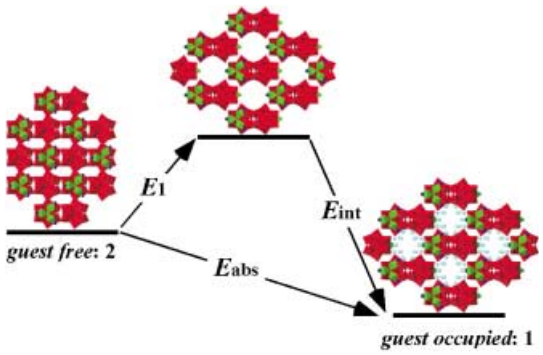

Figure 5. Schematic model of energy changes of the host ionic crystal upon guest inclusion.

sorption energy ($E_{int}-E_1=E_{abs}$) becomes >0 and the guest molecule can be accommodated into the solid bulk. E_{int} between the host and the guest can be calculated according to the Equation (1), where Q, μ, and r are the charge of the constituent ion [C],[29] the dipole moment of the guest [debye], and the ion–dipole (host–guest) distance, respectively. ε_0 and N_A are the dielectric constant of vacuum ($8.854\times10^{-12}\,J^{-1}C^2m^{-1}$) and the Avogadro number ($6.022\times10^{23}\,mol^{-1}$), respectively.[30]

$$E_{int} = -\frac{Q\mu}{4\pi\varepsilon_0 r^2}\times N_A \qquad (1)$$

Thus, the ion–dipole interaction is proportional to the dipole moment of the guest and inversely proportional to the ion–dipole (host–guest) distance. The latter becomes larger with the increase in the number of carbon atoms in the guest molecule. Therefore, E_{int} increases with the decrease in the number of carbon atoms and the increase in the dipole moment of the guest molecule. Thus, the easy inclusion of small polar molecules into **2** can be quantitatively explained by these interactions.

Quantitative explanation of the inclusion of water: Next, the water sorption was investigated in more detail on the basis of Figure 5. E_{int} for the water sorption can be divided into three components since there were three kinds of constituent ions (K^+, $[Cr_3O(OOCH)_6(H_2O)_3]^+$, $[\alpha\text{-}SiW_{12}O_{40}]^{4-}$). The polyoxometalate ($r\approx0.5$ nm) and macrocation ($r\approx0.35$ nm) are much larger than K^+ ($r=0.152$ nm) and the ion–dipole interaction energies are proportional to the square inverse of the ion–dipole distance. The former interaction energies were less than 10% of that for K^+ ($-357\,kJ\,mol^{-1}$ (a)) and are probably negligible. However, water molecules possess hydroxy groups and can additionally interact with the oxygen atoms of the polyoxometalate or the macrocation through hydrogen bonding. Therefore, the interaction of water molecules with the oxygen atom of the polyoxometalate ($-119\,kJ\,mol^{-1}$ (b)) or macrocation ($-266\,kJ\,mol^{-1}$ (c)) were also considered. The sum (E_{int}) of the host–guest interaction energies for (a), (b), and (c) was $-742\,kJ\,mol^{-1}$.[31]

E_{abs} was estimated from the water sorption isotherm at different temperatures by using the Clausius–Clapeyron equation.[32] Figure 6a shows the water sorption isotherms of

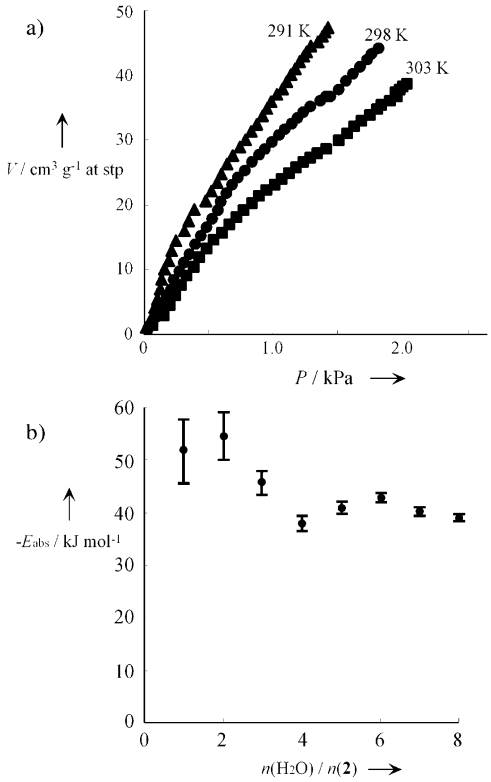

Figure 6. a) Water sorption isotherms of **2** at different temperatures. b) Water sorption energy of **2** calculated by using the Clausius–Clapeyron equation.

2. The water sorption energy calculated from the Clausius–Clapeyron equation is shown in Figure 6b. The total water sorption energy for **2** was estimated from the sum of energies for the 16 water molecules and a value of $E_{abs}=-519\pm20\,kJ\,mol^{-1}$ was obtained.[33] Therefore, the energy for the bulk expansion ($E_1=E_{int}-E_{abs}$) was $223\pm20\,kJ\,mol^{-1}$. In a separate way, E_1 could also be estimated by the difference in the lattice energies, since **1** and **2** are ionic crystals. The lattice energies of **1** and **2** can be estimated according to the equation of Glasser and Jenkins[34] and were approximately -2700 and $-2900\,kJ\,mol^{-1}$, respectively. Thus, E_1 was estimated to be approximately $200\,kJ\,mol^{-1}$. This value agrees fairly well with the value of $223\pm20\,kJ\,mol^{-1}$ and supports the idea that the E_1 values do not change much with the guests.

Gate pressure: The nature of the gate pressures in the case of C_2 guests was considered. If the potential energy of the guest molecule in the solid phase (E_s) was larger than that in the gas phase (E_g), the guest molecule would be included into the solid bulk. The gate pressure is a unique pressure where E_g is equal to E_s. The potential energy of the included guest (E_s) can be described as in Equation (2), where μ_s is the chemical potential of the liquid guest.[35,36]

$$E_s = E_{int} + \mu_s - E_1 \quad (2)$$

Since E_{int}, μ_s, and E_1 are independent of the gas pressure, E_s is also independent of the gas pressure. On the other hand, the potential energy or the chemical potential of the guest molecule in the gas phase is defined as in Equation (3),[37] where $P°$ is 1 atm (101.3 kPa) and $\mu_g°$ is the chemical potential of the molecule in the gas phase at standard state (1 atm, 298 K). Since E_g decreases with the increase in P, the guest inclusion becomes favorable at high gas pressures.

$$E_g = \mu_g = \mu_g^o + RT\ln(P/P^o) \quad (3)$$

Here we attempted to calculate E_s and E_g values upon inclusion of 16 water molecules into **2**. From Equation (2), E_s was calculated to be $-4314\ kJ\,mol^{-1}$ since E_1 and E_{int} were 223 and $-742\ kJ\,mol^{-1}$, respectively, and $\mu_s°$ for water was reported to be $-237.18\ kJ\,mol^{-1}$.[38] From Equation (3), E_g was calculated to be $(-3657+16RT\ln(P/P_0))\ kJ\,mol^{-1}$, since $\mu_g°$ for water was reported to be $-228.59\ kJ\,mol^{-1}$.[38] Therefore, E_g is equal to E_s at $P=6.44\times10^{-3}$ Pa (gate pressure). The value was almost zero and agreed with the fact that the water sorption started at very low pressure, as shown in Figure 3.

In the case of ethanol, $\mu_s°$ ($-174.2\ kJ\,mol^{-1}$) and $\mu_g°$ ($-168.3\ kJ\,mol^{-1}$) values have been reported.[38] On the assumption that the E_1 value for ethanol sorption is the same as that for water sorption and that the position of ethanol included is the same as that of water included, the gate pressure is estimated to be 2.88 kPa.[39] This value agrees fairly well with the experimental value of approximately 3.3 kPa.[12]

Selective oxidation of mixed alcohols: The inclusion properties of **2** were reflected in the oxidation of a mixture of alcohols with hydrogen peroxide. Oxidation of the alcohols did not proceed when $K_4[\alpha\text{-}SiW_{12}O_{40}]$ (heterogeneous phase) or $(TBA)_4[\alpha\text{-}SiW_{12}O_{40}]$ (homogeneous phase; TBA = tetrabutylammonium) were added, while addition of $[Cr_3O(OOCH)_6(H_2O)_3](OOCH)$ (homogeneous phase) produced 75 μmol of formaldehyde and 100 μmol of acetaldehyde. These facts show that the macrocation ($[Cr_3O(OOCH)_6(H_2O)_3]^+$) in **2** is the active species for the oxidation of alcohols. Figures 7a and b show changes in the concentrations of the aldehydes and alcohols, respectively, as a function of time. The concentration of methanol initially decreased while that of ethanol started to decrease after a short induction period (0.5 h). These concentrations of alcohols reached constant values after about 2 h. The concentration of formaldehyde increased after 1 h and reached a constant value of 35 μmol after 9 h, while the concentration of acetaldehyde was negligible. No hydrogen peroxide was detected after 9 h. Therefore, the oxidation was completed after 9 h. After the complete consumption of hydrogen peroxide, the amounts of alcohols, aldehydes, and water were confirmed by the dissolution of **2** by addition of acetonitrile into the reaction solution. The amounts of methanol, ethanol, formaldehyde, acetaldehyde, and water retained in **2** were 200, 70, 7, 0, and 500 μmol, respectively. These results show that only methanol is oxidized to formaldehyde and no oxidation of ethanol occurs. Thus, the selective oxidation of methanol could be achieved by the utilization of the selective inclusion properties of **2**. The sum of the amount of formaldehyde produced was 42 μmol and the turnover number was 0.84 on the assumption that the whole macrocation is effective for the oxidation. The inclusion of ethanol under the oxidation conditions is probably caused by the presence of water in aqueous 30% hydrogen peroxide (H_2O, 580 μmol; H_2O_2, 250 μmol). In fact, when 1.50 mmol of water was added to the 1,2-dichloroethane solution (4 mL) containing 1.50 mmol of ethanol and 50 μmol of **2**, the ethanol uptake reached approximately 0.8 molecules per **2**, while ethanol was excluded without the addition of water.

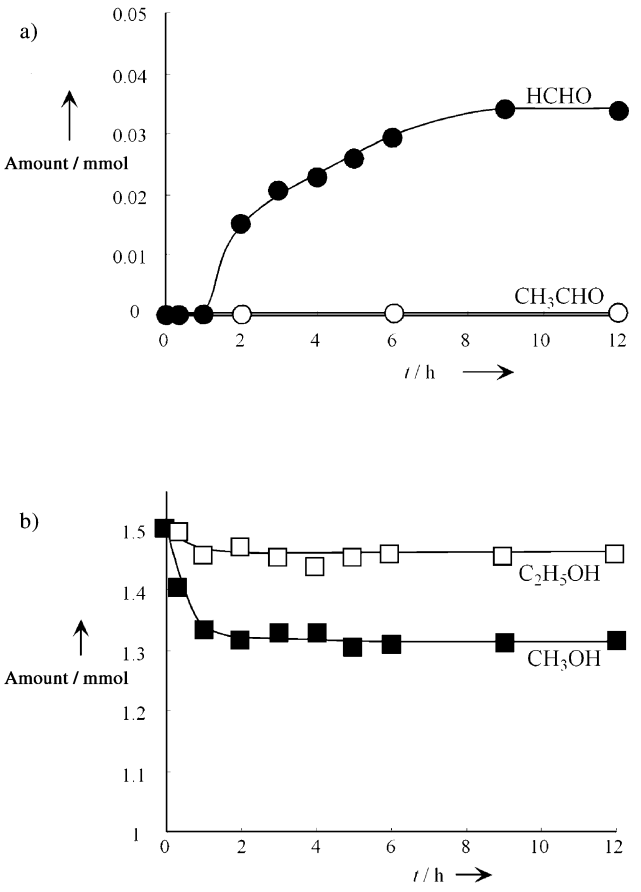

Figure 7. Time courses of alcohol oxidation by **2** at 298 K. Changes in a) aldehyde and b) alcohol concentrations. Initial conditions: 0.175 g (50 μmol) of **2**, 1.50 mmol of methanol and ethanol, and 0.25 mmol of 30% H_2O_2 in 1,2-dichloroethane (4 mL, 50 mmol).

Conclusion

A microstructured ionic crystal $K_3[Cr_3O(OOCH)_6(H_2O)_3][\alpha\text{-}SiW_{12}O_{40}]\cdot 16H_2O$ (**1**) was synthesized by the complexation of Keggin-type polyoxometalate and a large macrocation. The water of crystallization in **1** was easily removed under vacuum to form a guest-free phase **2**. Compound **2** reversibly absorbed water and polar organic molecules with two carbons or less. The unique inclusion properties of **2** could be quantitatively explained by the magnitude of the ion–dipole interaction between the host and the guest. This guest-inclusion property was successfully applied to the selective oxidation of a mixture of alcohols. These results could first be achieved by rationally designed ionic crystals.

Experimental Section

Synthesis of ionic crystals: A crystalline sample of $K_3[Cr_3O(OOCH)_6(H_2O)_3][\alpha\text{-}SiW_{12}O_{40}]\cdot 16H_2O$ (**1**) was synthesized by using our published procedure.[12] CCDC-160502 contains the crystallographic data for **1**. These data can be obtained free of charge via www.ccdc.cam.ac.uk/conts/retrieving.html (or from the Cambridge Crystallographic Data Centre, 12 Union Road, Cambridge CB2 1EZ, UK; fax: (+44) 1223-336033; or deposit@ccdc.cam.uk). Compound **2** was prepared by evacuation of **1** at room temperature.

$K_3[Fe_3O(OOCH)_6(H_2O)_3][\alpha\text{-}SiW_{12}O_{40}]\cdot 16H_2O$ (**3**): $K_4[\alpha\text{-}SiW_{12}O_{40}]\cdot n H_2O$[17] (1.0 g, 0.30 mmol) and $[Fe_3O(OOCH)_6(H_2O)_3](NO_3)\cdot n H_2O$[18] (0.33 g, ca 0.6 mmol) were dissolved into dilute aqueous HCOOH (30 mL, pH 1.8). KCl (0.8 g, 10.7 mmol) was then added. The solution was filtered after 30 min and the filtrate was kept at 6 °C for 2–3 days. Red crystals of **3** were isolated in approximately 70% yield. IR (KBr): $\tilde{\nu}$ = 1617 (vs, ν_{asym}(OCO)), 1370 (vs, ν_{sym}(OCO)), 981 (s, ν_{asym}(W=O)), 929 (br, ν_{asym}(Si–O)), 885 (m, ν_{asym}(W–O_c–W)), 791 (br, ν_{asym}(W–O_e–W)) cm^{-1}; elemental analysis: calcd for $C_6H_{44}Fe_3K_3O_{72}SiW_{12}$: Fe 4.42, K 3.09, Si 0.74, W 58.26; found: Fe 4.40, K 3.25, Si 0.80, W 59.00.

$K_3[Cr_3O(OOCH)_6(H_2O)_3][\alpha\text{-}PVW_{11}O_{40}]\cdot 16H_2O$ (**4**): $K_4[\alpha\text{-}PVW_{11}O_{40}]\cdot n H_2O$[40] (1.1 g, 0.37 mmol) and $[Cr_3O(OOCH)_6(H_2O)_3](OOCH)\cdot n H_2O$[18] (0.22 g, 0.4 mmol) were dissolved into dilute aqueous HNO_3 (30 mL, pH 2.0). KCl (0.8 g, 10.7 mmol) was then added. The solution was filtered after 30 min and the filtrate was kept at 6 °C for 1–2 days. Yellow-green crystals of **4** were isolated in approximately 70% yield. IR (KBr): $\tilde{\nu}$ = 1635 (vs, ν_{asym}(OCO)), 1377 (vs, ν_{sym}(OCO)), 1099, 1078 (m, ν_{asym}(P–O)), 1065 (sh, ν_{asym}(P–O)), 983 (s, ν_{asym}(W=O)), 885 (m, ν_{asym}(W–Oc–W)), 793 (br, ν_{asym}(W–Oe–W)), 660 (m, ν_{asym}(Cr_3–O)) cm^{-1}; elemental analysis: calcd for $C_6H_{44}Cr_3K_3O_{72}PVW_{11}$: Cr 4.28, K 3.20, P 0.85, V 1.39, W 55.48; found: Cr 4.25, K 3.15, P 0.83, V 1.37, W 55.16.

Physical measurements: FT-IR spectra were recorded from KBr pellets with a Paragon 1000 PC (Perkin Elmer) spectrometer. Diffuse reflectance UV/Vis spectra were recorded with a Lambda 12 (Perkin Elmer) spectrometer with $BaSO_4$ as a standard. TG measurements were performed with a SSC5200H instrument (Seiko Instruments) with α-Al_2O_3 as a reference under N_2 flow (300 mL min^{-1}). Solid-state MAS NMR spectra were recorded with a Chemagnetics CMX-300 Infinity spectrometer operating at 7.05 T (300 MHz). The resonance frequencies for ^1H and ^{13}C were 300.51 and 75.57 MHz, respectively. Compound **2** with a known amount of alcohol guests was transferred to a glass cell and sealed. The cell was set into a zirconia rotor and spun at a MAS rate of 3–5 kHz. XRD measurements with controlled water vapor pressure (N_2 balance) were carried out with an XRD-DSCII instrument (Rigaku Corporation) under the following conditions: $Cu_{K\alpha}$ radiation (50 kV-200 mA), 2θ = 4–38°, scan rate of 3° min^{-1}. The equilibrium of the water sorption was confirmed by the fact that the DSC curve showed no endothermic or exothermic peaks and the XRD pattern remained unchanged.

Sorption measurements: The gas sorption isotherms of **2** were measured with an automatic Omnisorp 100CX sorption apparatus (Coulter corporation). P_0 is the saturation pressure of the sorbents at 298 K, as follows: Nitrogen monoxide 101.3, methane 101.3, methanol 15.6, ethanol 6.67, 1-propanol 2.67, 1-butanol 1.35, acetonitrile 10.7, propionitrile 6.27, butylonitrile 2.67, formic acid 4.80, and acetaldehyde 101.3 kPa. The N_2 sorption isotherm at 77 K (P_0 = 101.3 kPa) was measured with an ASAP 2000 gas analyzer (Micromeritics).

Oxidation of alcohols: 30% H_2O_2 (0.25 mmol) was added to the mixture of methanol (1.50 mmol) and ethanol (1.50 mmol) in 1,2-dichloroethane (4 mL, 50 mmol). Compound **2** (0.175 g, 5.0×10^{-2} mmol) was added to the solution but was insoluble, so a heterogeneous mixture was formed. Concentrations of alcohols and their oxidative products were detected by GC (Shimadzu GC-8A model with Porapak QS and N columns and a TCD detector).

Acknowledgement

Mr. A. Kishi of Rigaku Corporation is acknowledged for providing advice for the measurements depicted in Figure 2. This work was supported in part by the Core Research for Environmental Science and Technology (CREST) program of the Japan Science and Technology Corporation (JST) and a Grant-in-Aid for scientific research from the Ministry of Education, Sports, Science, and Technology of Japan.

[1] a) S. M. Csicsery, *Pure Appl. Chem.* **1986**, *56*, 841; b) A. Corma, *Chem. Rev.* **1995**, *95*, 559; c) W. E. Farneth, R. J. Gorte, *Chem. Rev.* **1995**, *95*, 615; d) R. A. van Santen, G. J. Kramer, *Chem. Rev.* **1995**, *95*, 637; e) A. K. Cheetham, G. Férey, T. Loiseau, *Angew. Chem.* **1999**, *111*, 3466; *Angew. Chem. Int. Ed.* **1999**, *38*, 3268; f) J. M. Thomas, *Angew. Chem.* **1999**, *111*, 3852; *Angew. Chem. Int. Ed.* **1999**, *38*, 3588.

[2] a) M. Fujita, Y. J. Kwon, S. Washizu, K. Ogura, *J. Am. Chem. Soc.* **1994**, *116*, 1151; b) S. Kitagawa, M. Kondo, *Bull. Chem. Soc. Jpn.* **1998**, *71*, 1739; c) J. S. Seo, D. Whang, H. Lee, S. I. Jun, J. Oh, Y. J. Jeon, K. Kim, *Nature* **2000**, *404*, 982; d) M. Eddaoudi, D. B. Moler, H. Li, B. Chen, T. M. Reinke, M. O'Keeffe, O. M. Yaghi, *Acc. Chem. Res.* **2001**, *34*, 319; e) B. Moulton, M. J. Zaworotko, *Chem. Rev.* **2001**, *101*, 1629; f) B. Gomez-Lor, E. Gutierrez-Puebla, M. Iglesias, M. A. Monge, C. Ruiz-Valero, N. Snejko, *Inorg. Chem.* **2002**, *41*, 2429; g) L. Pan, H. Liu, X Lei, X. Huang, D. H. Plson, N. J. Turro, J. Li, *Angew. Chem.* **2003**, *115*, 560; *Angew. Chem. Int. Ed.* **2003**, *42*, 542.

[3] a) K. Endo, T. Sawaki, M. Koyanagi, K. Kobayashi, H. Masuda, Y. Aoyama, *J. Am. Chem. Soc.* **1995**, *117*, 8341; b) T. Hertzsch, F. Budde, E. Weber, J. Hulliger, *Angew. Chem.* **2002**, *114*, 2385; *Angew. Chem. Int. Ed.* **2002**, *41*, 2282.

[4] a) M. Albrecht, M. Lutz, A. L. Spek, G. van Koten, *Nature* **2000**, *406*, 970; b) M. Albrecht, R. A. Gossage, M. Lutz, A. L. Spek, G. van Koten, *Chem. Eur. J.* **2000**, *6*, 1431; c) K. M. Padden, J. F. Krebs, C. E. MacBeth, R. C. Scarrow, A. S. Borovik, *J. Am. Chem. Soc.* **2001**, *123*, 1072.

[5] a) V. A. Russell, C. C. Evans, W. Li, M. D. Ward, *Science* **1997**, *276*, 575; b) C. J. Kepert, D. Hesek, P. D. Beer, M. J. Rosseinsky, *Angew. Chem.* **1998**, *110*, 3335; *Angew. Chem. Int. Ed.* **1998**, *37*, 3158; c) A. J. Fletcher, E. J. Cussen, T. J. Prior, M. J. Rosseinsky, C. J. Kepert, K. M. Thomas, *J. Am. Chem. Soc.* **2001**, *123*, 10001; d) M. Edgar, R. Mitchell, M. Z. Slawin, P. Lightfoot, P. A. Wright, *Chem. Eur. J.* **2001**, *7*, 5168; e) R. Kitaura, K. Fujimoto, S. Noro, M. Kondo, S. Kitagawa, *Angew. Chem.* **2002**, *114*, 141; *Angew. Chem. Int. Ed.* **2002**, *41*, 133; f) E. J. Cussen, J. B. Claridge, M. J. Rosseinsky, C. J. Kepert, *J. Am. Chem. Soc.* **2002**, *124*, 9574.

[6] a) O. M. Yaghi, G. Li, H. Li, *Nature* **1995**, *378*, 703; b) K. Biradha, Y. Hongo, M. Fujita, *Angew. Chem.* **2002**, *114*, 3545; *Angew. Chem. Int. Ed.* **2002**, *41*, 3395.

[7] a) M. T. Pope, A. Müller, *Angew. Chem.* **1991**, *103*, 56; *Angew. Chem. Int. Ed. Engl.* **1991**, *30*, 34; b) T. Okuhara, N. Mizuno, M. Misono, *Adv. Catal.* **1996**, *41*, 113; c) "Polyoxometalates" (Ed.: C. L. Hill): *Chem. Rev.* **1998**, *98*, 1; d) R. Neumann, *Prog. Inorg. Chem.* **1998**, *47*, 317.

[8] a) M. Misono, N. Mizuno, K. Katamura, A. Kasai, Y. Konishi, K. Sakata, T. Okuhara, Y. Yoneda, *Bull. Chem. Soc. Jpn.* **1982**, *55*, 400; b) J. G. Highfield, J. B. Moffat, *J. Catal.* **1985**, *95*, 108; c) J. G. Highfield, J. B. Moffat, *J. Catal.* **1986**, *98*, 245; d) T. Okuhara, S. Tatemateu, K. W. Lee, M. Misono, *Bull. Chem. Soc. Jpn.* **1989**, *62*, 717; e) J. B. Moffat, *Metal–Oxygen Clusters*, Kluwer Academic/Plenum, New York, **2001**, chap. 7.

[9] a) N. Mizuno, M. Misono, *Chem. Lett.* **1987**, 267; b) T. Okuhara, T. Nishimura, M. Misono, *Chem. Lett.* **1995**, 155; c) Y. Yoshinaga, K. Seki, T. Nakato, T. Okuhara, *Angew. Chem.* **1997**, *109*, 2946; *Angew. Chem. Int. Ed. Engl.* **1997**, *36*, 2833.

[10] a) M. Hölscher, U. Englert, B. Zibrowius, W. F. Hölderich, *Angew. Chem.* **1994**, *106*, 2552; *Angew. Chem. Int. Ed. Engl.* **1994**, *33*, 2491; b) A. Müller, E. Krickemeyer, H. Bögge, M. Schmidtmann, F. Peters, C. Menke, J. Meyer, *Angew. Chem.* **1997**, *109*, 500; *Angew. Chem. Int. Ed. Engl.* **1997**, *36*, 484; c) M. I. Khan, E. Yohannes, D. Powell, *Inorg. Chem.* **1999**, *38*, 212; d) D. Hagrman, P. J. Hagrman, J. Zubieta, *Angew. Chem.* **1999**, *111*, 3359; *Angew. Chem. Int. Ed.* **1999**, *38*, 3165; e) J. H. Son, H. Choi, Y. U. Kwon, *J. Am. Chem. Soc.* **2000**, *122*, 7432; f) A. Müller, E. Krickemeyer, H. Bögge, M. Schmidtmann, P. Kögerler, C. Rosu, E. Beckman, *Angew. Chem.* **2001**, *113*, 4158; *Angew. Chem. Int. Ed.* **2001**, *40*, 4034.

[11] a) V. W. Day, W. G. Klemperer, O. M. Yaghi, *J. Am. Chem. Soc.* **1989**, *111*, 5959; b) M. I. Khan, J. Zubieta, *Angew. Chem.* **1994**, *106*, 784; *Angew. Chem. Int. Ed. Engl.* **1994**, *33*, 760; c) Y. Hayashi, F. Müller, Y. Lin, S. M. Miller, O. P. Anderson, R. G. Finke, *J. Am. Chem. Soc.* **1997**, *119*, 11401.

[12] S. Uchida, M. Hashimoto, N. Mizuno, *Angew. Chem.* **2002**, *114*, 2938; *Angew. Chem. Int. Ed.* **2002**, *41*, 2814.

[13] A. Kobayashi, Y. Sasaki, *Bull. Chem. Soc. Jpn.* **1975**, *48*, 885.

[14] a) B. N. Figgis, G. B. Robertson, *Nature* **1965**, *205*, 694; b) S. C. Chang, G. A. Jeffrey, *Acta Crystallogr. Sect. B* **1970**, *26*, 673. These references contain the crystal structure of the Cr^{III} cation with acetate bridges, $[Cr_3O(OOCCH_3)_6(H_2O)_3]^+$. As far as we know, the crystal structure of **1** is the first case of the formate analogue.

[15] The volume of the channel was estimated by considering the ionic radii (Cr^{3+}, K^+) and van der Waals radii (other atoms) of the constituent ions.

[16] The details of the syntheses of $K_3[Fe_3O(OOCH)_6(H_2O)_3][\alpha\text{-}SiW_{12}O_{40}]\cdot 16H_2O$ (**3**) and $K_3[Cr_3O(OOCH)_6(H_2O)_3][\alpha\text{-}PVW_{11}O_{40}]\cdot 16H_2O$ (**4**) are presented in the Experimental Section. **1**, **3**, and **4** gave identical XRD patterns (as shown in Figure S-1 in the Supporting Information), a result indicating that the preservation of the charge and shape of the constituent ions is requisites for the construction of the channeled structure.

[17] A. Tézé, G. Hervé, *Inorg. Syn.* **1990**, *27*, 93.

[18] M. K. Johnson, D. B. Powell, R. D. Cannon, *Spectrochim. Acta* **1981**, *37A*, 995.

[19] The oxygen to tungsten charge transfer band of the α Keggin structure appeared at 270 nm. $^4A_{2g}\rightarrow{}^4T_{1g}$ and $^4A_{2g}\rightarrow{}^4T_{2g}$ of the octahedral Cr^{III} d–d transition of the trinuclear Cr^{II} configuration appeared at 440 and 580 nm, respectively.

[20] G. C. Pimentel, A. L. McClellan, *The Hydrogen Bond*, W. H. Freeman and Company, San Francisco, **1960**, chap. 3.

[21] The experimental XRD pattern of **2** was well reproduced by the calculation based on the idealized closest packing with a coherent length of a unit cell, which indicates only short-range ordering of the ions. A similar closest packing was observed for the complex of the Keggin-type polyoxometalate $[\alpha\text{-}CoW_{12}O_{40}]^{6-}$ with $[Cr_3O(OOCH)_6(H_2O)_3]^+$. The channel volume of this complex was 17% of the unit cell, which was comparable to the ideal closest-packing model of **2** (20%). The details will be described in a subsequent article.

[22] In Figure 2, the diffraction peak at the lowest angle monotonically shifted from $2\theta = 9.0\pm0.1°$ to $8.0\pm0.1°$in the range of $P/P_0 = 0$–0.8, which corresponds to a lattice volume increase of approximately 2000 Å^3. This value agrees fairly well with the value of 1500 Å^3 calculated from the fact that 12 water molecules were included at $P/P_0 = 0.8$ in Figure 3 and the Z value was 4.

[23] Exposure of **2** to methanol vapor gave an XRD pattern analogous to that of $K_2[Cr_3O(OOCH)_6(H_2O)_{2.5}(CH_3OH)_{0.5}]_2[\alpha\text{-}SiW_{12}O_{40}]\cdot E8\text{-}CH_3OH$. Crystallographic data: Orthorhombic $Pna2_1$, $a = 24.796(6)$, $b = 15.406(3)$, $c = 22.042(5)$, $Z = 4$, $R_1 = 0.0480$, $wR2 = 0.0480$. See ref. [12] for further information.

[24] S. J. Gregg, K. S. W. Sing, *Adsorption, Surface Area and Porosity*, Academic Press, London, **1982**, p. 237.

[25] a) R. W. Mooney, A. G. Keenan, L. A. Wood, *J. Am. Chem. Soc.* **1952**, *74*, 1367; b) R. M. Barrer, D. M. MacLeod, *Trans. Faraday Soc.* **1954**, *50*, 980; c) S. Yamanaka, F. Kanamaru, M. Koizumi, *J. Phys. Chem.* **1974**, *78*, 42.

[26] A. L. McClellan, *Tables of Experimental Dipole Moments*, W. H. Freeman and Company, San Francisco, **1963**.

[27] a) D. Li, K. Kaneko, *Chem. Phys. Lett.* **2001**, *335*, 50; b) R. Kitaura, K. Fujimoto, S. Noro, M. Kondo, S. Kitagawa, *Angew. Chem.* **2002**, *114*, 141; *Angew. Chem. Int. Ed.* **2002**, *41*, 133.

[28] a) C. Tsiao, D. R. Corbin, C. Dybowski, *J. Am. Chem. Soc.* **1990**, *112*, 7140; b) E. J. Munson, A. A. Kheir, N. D. Lazo, J. F. Haw, *J. Phys. Chem.* **1992**, *96*, 7740.

[29] Charges of -2 and -0.5 were used for the oxygen atoms of the polyoxometalate and macrocation, respectively, in the calculation of the ion–dipole interaction with water molecules. The dipole moment of the water molecule found in ref. [26] was 1.85 debye.

[30] P. W. Atkins, *Physical Chemistry*, Oxford University Press, Oxford, **1990**, chap. 22.

[31] The entropy term of E_{int} was considered to be negligible according to the following calculation. A gaseous molecule looses the translational freedom ($3/2kT$) after being absorbed into the solid host. Thus, the maximum entropy loss upon the sorption of 16 water molecules into **2** was calculated to be 59.5 kJ mol^{-1}, which is only 8% of the E_{int} value (-742 kJ mol^{-1}).

[32] P. W. Atkins, *Physical Chemistry*, Oxford University Press, Oxford, **1990**, chap. 29.

[33] The sorption energies of the 16 water molecules per **2**, obtained from the Clausius–Clapeyron plots, were added and a total value of -519 ± 20 kJ mol^{-1} was obtained.

[34] L. Glasser, H. D. B. Jenkins, *J. Am. Chem. Soc.* **2000**, *122*, 632.

[35] The water sorption energy of **2** was comparable to the heat of condensation of -44 kJ mol^{-1} at 298 K (as shown in Figure 6b) and the volume occupied by one molecule of the water of crystallization in **1** was close to that of liquid water. Therefore, the chemical potential of the included guests may be close to that in the liquid state. A similar treatment has been reported for clays. See ref. [36].

[36] a) A. Delville, *Langmuir* **1991**, *7*, 547; b) R. M. Shroll, D. E. Smith, *J. Chem. Phys.* **1999**, *111*, 9025.

[37] P. W. Atkins, *Physical Chemistry*, Oxford University Press, Oxford, **1990**, chap. 5.

[38] D. R. Stull, E. F. Westrum, Jr., G. C. Sinke, *The Chemical Thermodynamics of Organic Compounds*, John Wiley and Sons, New York, **1969**.

[39] The dipole moments of water and ethanol were 1.85 and 1.68 debye, respectively, according to ref. [26]. The cross-molecular areas of water and ethanol estimated from the liquid density at 298 K were 0.105 and 0.230 nm^2, respectively.

[40] P. J. Domaille, *Inorg. Syn.* **1990**, *27*, 96.

Received: February 21, 2003
Revised: July 28, 2003 [F4874]

